

## Convective Circulations Induced by Surface Heterogeneities

ENIO P. SOUZA\* AND NILTON O. RENNÓ

*Department of Atmospheric Sciences, The University of Arizona, Tucson, Arizona*

MARIA A. F. SILVA DIAS

*Departamento de Ciências Atmosféricas, Universidade de São Paulo, São Paulo, Brazil*

(Manuscript received 16 December 1998, in final form 1 October 1999)

### ABSTRACT

A simple theory for convective circulations induced by surface heterogeneities is proposed. The theory is based on the thermodynamics of heat engines and provides a simple physical explanation for the general characteristics of circulations forced by surface inhomogeneities in sloping terrains. In particular, the theory is applied to a mesoscale circulation induced by deforestation. It predicts that the intensity of the mesoscale convective circulation forced by deforestation depends on the difference of the near-surface nonadiabatic temperature and humidity between the forest and cleared regions and on the depth of the convective boundary layer. The theory was successfully tested against observations made during a field experiment in the Amazon forest and a nearby clearing.

### 1. Introduction

Local circulations might occur when a temperature difference is established between two regions. The sea-land breeze and the valley–mountain circulation are examples of these thermally direct circulations (Atkinson 1981; Rotunno 1983; Pielke 1984; Dalu and Pielke 1989). In general, horizontal temperature gradients are a consequence of differential heating of the surface. Numerical simulations (e.g., Pielke 1974; Mahrer and Pielke 1977; Avissar and Pielke 1989) show that mesoscale circulations similar to the sea breeze can be forced by surface heterogeneities. When part of a forest is cleared, changes in the surface energy budget do occur. When the clearing is large enough to maintain a substantial temperature difference between the forest and the cleared region, a convective circulation between the two regions may occur. We show observational evidence of a mesoscale circulation between the native forest and a cleared area of the Amazon region. Numerical experiments by Silva Dias and Regnier (1996) also show evidence of this mesoscale circulation.

Rabin et al. (1990) observed that shallow cumulus clouds form earlier over areas of harvested wheat than over adjacent and colder areas covered by growing vegetation. Cutrin et al. (1995) observed an increase in the frequency of shallow cumulus clouds over areas in which the Amazon forest had been cleared. Moreover, they observed that the increase in the frequency of shallow cumulus clouds occurs only in the afternoon, that is, only when the air temperature is substantially higher over the cleared areas than over the forest. These observations suggest that there is a mesoscale convective circulation between the areas covered by vegetation and the cleared regions.

We propose a thermodynamical theory for the intensity of mesoscale circulations induced by surface heterogeneities in sloping terrains. The theory is based on the heat engine framework. This framework has been applied to the study of atmospheric vortices such as hurricanes (Emanuel 1986), Arctic lows (Emanuel 1989), and dust devils (Rennó et al. 1998). Moreover, Rennó and Ingersoll (1996) used the heat engine framework to study natural convection and to propose a theory for convective available potential energy (CAPE).

We use data from a field experiment in the Amazon forest and a nearby clearing (pasture) to test our theory for mesoscale circulations forced by surface heterogeneities. We show that during the day, the difference in surface pressure between the forest and the nearby pasture is systematically larger than the hydrostatic value due to the difference in height between the two sites.

---

\* Permanent affiliation: Departamento de Ciências Atmosféricas, Universidade Federal da Paraíba, Campina Grande, Brazil.

---

*Corresponding author address:* Prof. Nilton O. Rennó, Department of Atmospheric Sciences, The University of Arizona, P.O. Box 210081, Tucson, AZ 85721.  
E-mail: renno@atmo.arizona.edu

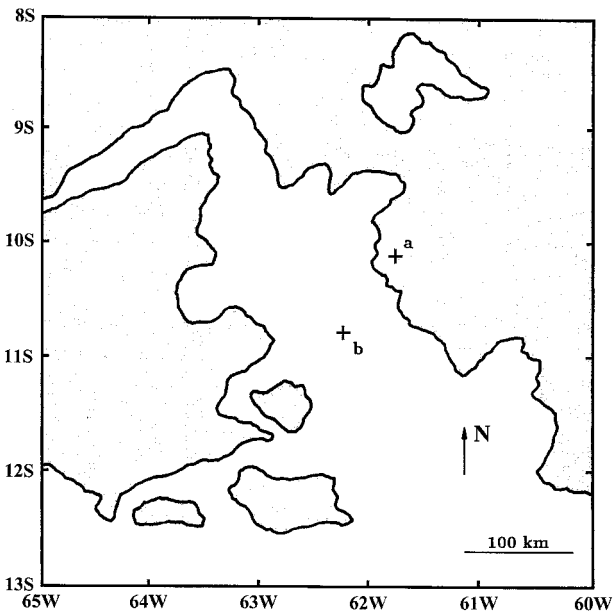


FIG. 1. The RBLE 3 experimental area is located in the state of Rondônia, Brazil, at approximately 10°S and 62°W. The locations of the forest and pasture observation sites (points a and b) are indicated in the figure. The white area is the region in which the forest was cleared.

Moreover, we show that the mesoscale circulation between the forest and the pasture is strongest between 1100 and 1400 local time (LT), that is, when the surface heat flux is near its peak diurnal value and the convective boundary layer is deep. We show that these observations, as well as the intensity of the circulation between the forest and the pasture, are consistent with the predictions of the proposed theory. We also use data from a field experiment on sea breezes in a sloping terrain (Silva Dias and Machado 1997) to test our theory. We show that the theory correctly predicts the non-hydrostatic pressure difference across the sea breeze front.

## 2. Observations

During Part 3 of the Rondonian Boundary Layer Experiment (RBLE 3), near-surface and upper-air data were simultaneously collected in a region of native forest (Reserva Jarú) and a clearing located at about 80 km to the southwest of the forest site (a pasture in Fazenda Nossa Senhora). Gash et al. (1996) describes the RBLE 3 experiment and datasets. The location of the two observational sites is indicated in Fig. 1. We study the data collected during 14–23 August 1994, the peak of the dry season in the region. During this period, upper-air and surface observations were made at the two sites at 0500, 0800, 1100, 1400, 1900, and 2300 LT (LT = UTC - 4 h). The forest and the pasture sites are located at about 120 and 220 m above sea level. However, there is a considerable error in the estimation of

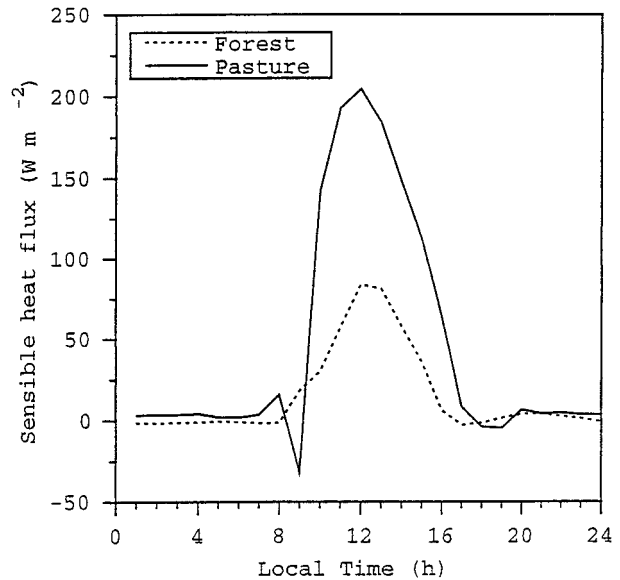


FIG. 2. Sensible heat flux observed over the forest and pasture sites. The displayed heat flux value is an average for the 10 days of the experiment.

the elevation of these two sites (G. Fisch 1998, personal communication). In order to correct difference in elevation between them, we assume that the difference of the mean tropospheric horizontal pressure is approximately zero between the two sites. Then, we compute the difference in elevation necessary to satisfy this condition. We conclude that the corrected difference in elevation between the two sites is  $\Delta z \approx 140$  m.

Figure 2 shows the time evolution of the sensible heat flux over the two sites. The energy available for dry (moist) convection is equal to the product of the sensible (total) heat flux to the thermodynamic efficiency (Rennó and Ingersoll 1996). The thermodynamic efficiency, in turn, is approximately proportional to the thickness of the convective boundary layer (Rennó et al. 1998). Thus, both the intensity of the circulation and the pressure drop between the two sites are maximum between 1100 and 1400 LT, when both the thermodynamic efficiency and the sensible heat flux are near their peak values. This occurs because, at this time, the energy available to do work is near its peak value, as discussed in section 4.

The convective circulation induced by deforestation (forest–pasture breeze) is superimposed on a synoptic-scale flow. In order to identify the convective circulation, we decompose the observed wind at a given observation time  $t$  into a time mean value plus a perturbation. That is, we take  $u = \bar{U} + u'$  and  $v = \bar{V} + v'$ , where  $\bar{U}$  and  $\bar{V}$  are the zonal mean and meridional mean components of the wind over the ten days of observation, and  $u'$  and  $v'$  are the perturbations at each observation time. In order to estimate the intensity of the circulation induced by deforestation, we compute the average wind perturbation for the ten days of ob-

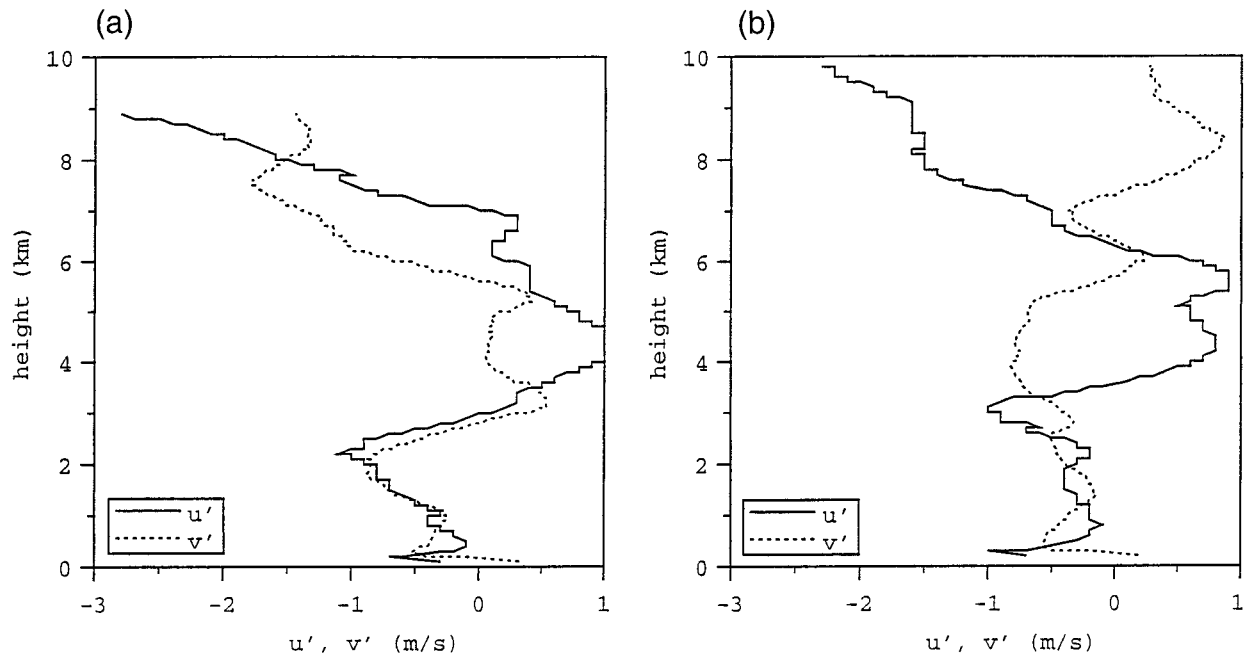


FIG. 3. Observed perturbation wind profile (a) over the forest and (b) over the pasture.

servation, at the times of peak surface heat fluxes (1100 and 1400 LT). Figure 3 shows the  $u'$  and  $v'$  components of the wind perturbation over the forest and pasture sites. Figure 3a shows that, at the time of strongest surface heat flux, the perturbation wind is directed from the forest to the pasture in the lowest 3 km of the atmosphere. Between 3 and 5 km above the surface, the perturbation wind is in the opposite direction. Figure 3b shows that the  $u$  component has a similar behavior over the pasture. Moreover, it shows that the forest–pasture breeze is weaker, noisier, and extends throughout a deeper layer over the pasture. We suggest that this happens because the sensible heat flux, and therefore the convective-driven turbulence, is stronger over the pasture.

The observation of a breeze from the forest to the pasture, at the times of peak surface heat flux, and the observation of a reversal in the wind direction above approximately 3 km suggest that there is a mesoscale circulation between the forest and the pasture. The numerical experiments of Silva Dias and Regnier (1996) support this idea. However, they also show that there is a weak circulation between the two sites even in the absence of deforestation. They speculate that this weak circulation is due to the fact that this is a region of sloping terrain, the pasture being higher than the native forest. When deforestation is included in the numerical simulation, a stronger circulation with maximum vertical velocity at the western edge of the pasture is observed.

We propose a theory for predicting the nonhydrostatic pressure drop between the forest and the pasture. Our theory supports the hypothesis that the mesoscale circulation between the two sites is partially induced by

deforestation. Moreover, it allows the quantification of the effects of deforestation versus sloping terrain on the intensity of the mesoscale circulation.

### 3. Theory

Emanuel (1986), Rennó and Ingersoll (1996), and Rennó et al. (1998) idealized hurricanes, atmospheric convection, and dust devils as reversible heat engines. In this study, we use the heat engine framework to formulate a simple theory for circulations driven by surface heterogeneities in sloping terrains. We apply the theory to both the study of a mesoscale convective circulation induced by deforestation and sea breezes in a sloping terrain.

An energy equation for a convecting air parcel follows from the dot product of the velocity vector and the equation of motion (Haltiner and Martin 1957). The resulting equation states that, following an air parcel in steady state,

$$d\left(\frac{1}{2}|\mathbf{v}|^2 + gz\right) + \alpha dp - \mathbf{f} \cdot d\mathbf{l} = 0, \quad (1)$$

where  $\mathbf{v}$  is the velocity vector,  $g$  the gravity acceleration,  $\alpha$  the specific volume,  $p$  the pressure,  $\mathbf{f}$  the frictional force per unit mass, and  $d\mathbf{l}$  is an increment distance along the air parcel's path. The steady-state and reversible process assumptions imply that our theory provides an upper bound for the intensity of the circulation. Note that the Coriolis acceleration term does not appear in Eq. (1) because the Coriolis force does not do work.

The integration of Eq. (1) along a closed circulation gives

$$\oint \alpha dp = \oint \mathbf{f} \cdot d\mathbf{l}, \quad (2)$$

which states that, in steady state, the work done by a convecting air parcel balances the frictional loss of energy.

Assuming that the process is reversible, the first and second laws of thermodynamics applied to moist air can be written as

$$Tds = d(c_p T + L_v r) - \alpha dp, \quad (3)$$

where  $T$  is the absolute air temperature,  $s$  the specific entropy,  $c_p$  the dry air specific heat,  $L_v$  the specific latent heat of vaporization, and  $r$  the water vapor mixing ratio. Integrating Eq. (3) along a closed circulation, we get

$$\oint T ds = -\oint \alpha dp = \oint p d\alpha. \quad (4)$$

Equation (4) states that, in steady state, the work done by the circulation is equal to the net heat input. It follows from Eqs. (2) and (4) that

$$\oint T ds = -\oint \mathbf{f} \cdot d\mathbf{l}. \quad (5)$$

This equation states that, in steady state, the net heat input balances the frictional loss of energy.

Integrating Eq. (1) along a near-surface streamline going from the forest (point a) to the pasture (point b), we get

$$\int_a^b \alpha dp \approx \int_a^b \mathbf{f} \cdot d\mathbf{l} - \int_a^b g dz, \quad (6)$$

where we have neglected changes in the kinetic energy that, in this study, are two orders of magnitude smaller than changes in the other terms.

Following Rennó et al. (1998) we define the fraction of the total dissipation of mechanical energy consumed by friction near the surface as

$$\gamma \equiv \frac{\int_a^b \mathbf{f} \cdot d\mathbf{l}}{\oint \mathbf{f} \cdot d\mathbf{l}}, \quad (7)$$

and the thermodynamic efficiency of the convective circulation as

$$\eta \equiv \frac{\oint T ds}{\int_a^b T ds}. \quad (8)$$

Since the intensity of the circulation is likely to be small, we neglect the contribution of the frictional heating to the heat input (see Rennó and Ingersoll 1996).

Combining Eqs. (5), (6), (7), and (8), we get

$$\int_a^b \alpha dp \approx -\gamma\eta \int_a^b T ds - \int_a^b g dz. \quad (9)$$

Integrating Eq. (3) near surface, from the forest (point a) to the pasture (point b), we get an expression for the total heat input

$$\int_a^b T ds = \int_a^b d(c_p T + L_v r) - \int_a^b \alpha dp. \quad (10)$$

Combining Eqs. (9) and (10), we get

$$(1 - \gamma\eta) \int_a^b \alpha dp \approx -\gamma\eta \int_a^b d(c_p T + L_v r) - \int_a^b g dz. \quad (11)$$

Neglecting changes in  $c_p$  and  $L_v$ , and using the ideal gas law, we get

$$p_b \approx p_a \exp \left\{ \frac{\gamma\eta}{(\gamma\eta - 1)R} \left[ \frac{c_p \Delta T}{\bar{T}_s} + \frac{L_v \Delta r}{\bar{T}_s} \right] + \frac{1}{(\gamma\eta - 1)R} \left[ \frac{g \Delta z}{\bar{T}_s} \right] \right\}, \quad (12)$$

where  $\Delta T = T_b - T_a$ ,  $\Delta r = r_b - r_a$  and  $\Delta z = z_b - z_a$  and where  $\bar{T}_s$  is the mean surface air temperature between points a and b.

The first term on the right-hand side of Eq. (12) is due to the absorption of sensible heat between the two points. This term represents the main physical process for producing sea-land breezes (e.g., Atkinson 1981; Pielke 1984) and dust devils Rennó et al. (1998). The second term represents the absorption of latent heat. This term is not important in dry convective systems, but it is the most important term in moist convective systems such as hurricanes (Emanuel 1986). The third term is a combination of the hydrostatic pressure drop due to the difference in height between points a and b (following an adiabat) and an upslope nonadiabatic expansion. This term will be discussed in more detail below. When the surface is assumed to be flat, Eq. (12) is identical to that derived by Rennó et al. (1998).

In order to better understand the physical mechanisms responsible for the upslope pressure drop, we divide the temperature difference between points a and b into adiabatic and nonadiabatic parts. We assume that no condensation occurs near the surface and take

$$\Delta T = \Delta T_{ad} + \Delta T_{na} = -\frac{g}{c_p} \Delta z + \Delta T_{na}, \quad (13)$$

where the subscripts ‘‘ad’’ and ‘‘na’’ stand for adiabatic and nonadiabatic parts, and where the temperature drop following a dry adiabat is given by  $\Delta T_{ad} = -(g/c_p)\Delta z$ .

Substituting Eq. (13) into Eq. (12), we get a simple expression for the pressure drop between points a and b, that is,

$$\Delta p \approx p_a \left\{ 1 - \exp \left[ \frac{\gamma \eta}{(\gamma \eta - 1)R} \left( \frac{c_p \Delta T_{na}}{T_s} + \frac{L_v \Delta r}{T_s} \right) - \frac{\Delta z}{H_s} \right] \right\}, \quad (14)$$

where  $\Delta p \equiv p_a - p_b$ ,  $\Delta T_{na} = T_b - T_a + (g/c_p)\Delta z$ , and  $H_s \equiv RT_s/g$  is a scale height.

Equation (14) predicts that the nonhydrostatic pressure drop, and therefore the intensity of a convective circulation in sloping terrain, depends on the thermodynamic efficiency of the circulation, the nonadiabatic temperature difference, and the difference in water vapor content between points a and b. Equation (14) suggests that topographical features induce convective circulations because they lead to nonadiabatic heating of the air parcels moving upslope.

One of the key parameters in Eq. (14) is the thermodynamic efficiency. It follows from Eq. (8) that the thermodynamic efficiency of the convective circulation can be written as

$$\eta \equiv \frac{\int_a^b T ds - \int_{out} T ds}{\int_a^b T ds} = \frac{T_h - T_c}{T_h}, \quad (15)$$

where  $T_h$  is the temperature of the hot reservoir and  $T_c$  is the temperature of the heat sink. It follows from the above that  $T_h$  and  $T_c$  are, respectively, the entropy-weighted average temperatures of the heat input (the surface air),  $T_h \equiv (\int_a^b ds)^{-1} \int_a^b T ds$ , and of the heat output (the convective boundary layer),  $T_c \equiv (\int_{out} ds)^{-1} \int_{out} T ds$ . Note that for a reversible heat engine  $\int_a^b ds = \int_{out} ds$  through a cycle (see Rennó et al. 1998). We take  $T_h$  as the mean surface air temperature between points a and b. Since most of the radiative cooling rate of convective layers, like those observed during the RBLE 3 field experiment (see Fig. 5), occurs near the top of the convective boundary layer (see Staley 1965), we take  $T_c$  as the temperature at this level. Thus, we have that

$$T_c \approx T_h - \Gamma_d Z, \quad (16)$$

where  $\Gamma_d = g/c_p$  is the dry adiabatic lapse rate and  $Z$  is the depth of the convective boundary layer. Combining Eqs. (15) and (16), the thermodynamic efficiency is given by

$$\eta \approx \frac{gZ}{c_p T_h}. \quad (17)$$

Equation (17) is equivalent to that derived by Golitsyn (1979) for a convective system in which the transfer of heat by convection is much greater than that by conduction.

The intensity of the thermally direct component of

TABLE 1. Observed difference between the near-surface air temperature over the pasture and forest sites ( $\Delta T = T_b - T_a$ ), observed depth of the convective boundary layer over the pasture ( $Z$ ), observed pressure drop between the forest and the pasture sites ( $\Delta p = p_a - p_b$ ), observed nonhydrostatic pressure drop between the forest and the pasture ( $\Delta p_{nh}$ ), and the calculated available energy flux ( $F_{av}$ ). All values are averages for the 10 days of observations.

Local time (hour)	0500	0800	1100	1400	1700	2300
$\Delta T$ (K)	-1.8	0.2	3.3	1.8	0.1	-1.0
$Z$ (m)	0.0	0.0	400	2000	2000	0.0
$\Delta p$ (hPa)	16.9	17.4	17.8	17.6	17.3	16.8
$\Delta p_{nh}$ (hPa)	0.8	1.4	1.8	2.0	1.6	0.8
$F_{av}$ ( $Wm^{-2}$ )	0.0	0.0	2.5	9.0	0.0	0.0

the mesoscale circulation can be determined independently of the pressure drop between points a and b. In the Tropics (e.g., in the RBLE 3 area), this is the main component of the circulation. Thus, following Rennó and Ingersoll (1996), the intensity of the convective circulation (forest–pasture breeze) is given by

$$|\mathbf{v}| \approx \left[ \frac{\eta}{\mu} (c_p \Delta T_{na} + L_v \Delta r) \right]^{1/2}, \quad (18)$$

where  $\mu$  is a dimensionless coefficient of dissipation of mechanical energy. Note that since the circulation is from higher to lower pressure, it is directed from the regions of lower (colder) to higher entropy (warmer). Thus, during the day, the direction of the forest–pasture breeze is from the forest to the pasture. It is important to note that our theory does not hold when neither moist nor dry convection is present. However, since these circulations lead to upward motion over the warm terrain, we believe that either dry or moist convection always occurs with the forest–pasture circulation. Equation (18) states that the intensity of the breeze is a function of the thermodynamic efficiency of the circulation and the nonadiabatic temperature and humidity differences between points a and b, and the magnitude of the coefficient of mechanical dissipation of energy.

#### 4. Results and discussion

The RBLE 3 occurred during the dry season in the Amazon region. Indeed, during the RBLE 3 field campaign, only nonprecipitating boundary layer convection was observed in the experimental area. Therefore, for this experiment we can neglect the latent heat terms in Eqs. (14) and (18). Moreover, during this experiment the heat input into the convective heat engine is equal to the sensible heat flux at the surface.

Table 1 shows the observed difference in near-surface air temperature between the pasture and forest sites ( $\Delta T = T_b - T_a$ ), the depth of the convective boundary layer over the pasture ( $Z$ ), the pressure drop between the forest and the pasture sites ( $\Delta p = p_a - p_b$ ), the nonhydrostatic pressure drop between the forest and the pasture ( $\Delta p_{nh}$ ), and the available energy turned into work

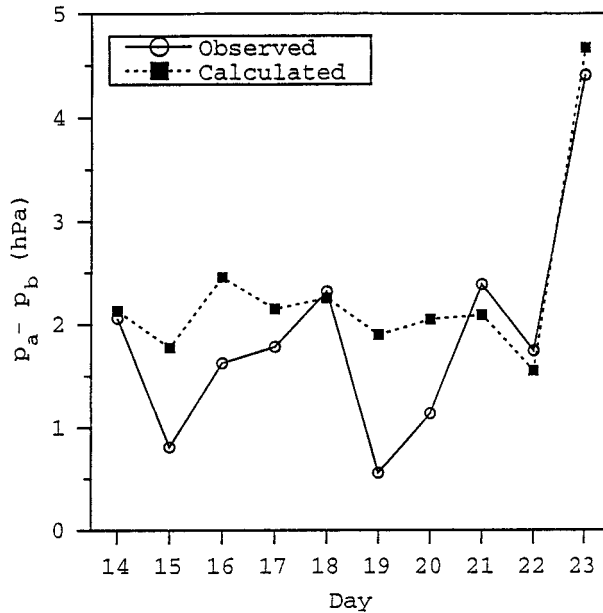


FIG. 4. Observed (full line) and computed (dashed line) nonhydrostatic pressure drop between the forest and the pasture sites.

by convection  $F_{av}$ . All values are averages for the 10 days of the experiment. Note that the nonhydrostatic pressure drop ranges from 0.8 to 2.0 hPa. Since the accuracy of the pressure measurements is about 0.3 hPa, the results presented in Table 1 suggest that some physical mechanism is responsible for the observed pressure drop between the forest and the pasture sites. The maximum value of the nonhydrostatic pressure drop between the forest and the pasture occurs at 1400 LT. It occurs at a time of large temperature difference between the forest and the pasture and large boundary layer depth. Note that at 1100 LT the boundary layer depth is much smaller than at 1400 LT, but the nonhydrostatic pressure drop is only slightly smaller. This happens because the temperature difference between the pasture and the forest is almost twice as large at 1100 as it is at 1400 LT. Alternatively, we can state that the maximum pressure drop occurs at the time at which the amount of work available from the convective heat engine ( $F_{av} = \eta F_{in}$ ) is near its peak value (see Rennó et al. 1998), where  $F_{in}$ , the surface sensible heat flux, is displayed in Fig. 2.

Figure 4 shows the observed and computed nonhydrostatic pressure drop at 1400 LT (the time of its peak value) for each day. Our theory predicts that the pressure drop from the forest to the pasture is of the same order of magnitude as the observed value. However, the predicted pressure drop is frequently larger than the observed value (e.g., during 16 and 19 August). We believe that this happens because we have assumed  $\gamma = 1$  in the computation of the nonhydrostatic pressure drop. Thus, what we have computed is an upper bound to the pressure drop. The temperature difference, as measured by an electronic sensor, is subject to a measurement error

TABLE 2. Observed values of the near-surface air temperature, the thermodynamic efficiency, and the nonhydrostatic pressure drop between the forest and the pasture at 1400 LT for each day of the field experiment. The observed thermodynamic efficiency was derived from the observed sounding over the pasture. The value of the nonhydrostatic pressure drop predicted by our theory is indicated between parentheses.

Day	$T_a$ (K)	$T_b$ (K)	$\eta$ (%)	$\Delta p$ (hPa)
14	302.9	304.6	5.8	2.1 (2.1)
15	304.0	305.2	5.8	0.8 (1.8)
16	303.9	306.1	5.7	1.6 (2.5)
17	303.3	304.7	6.4	1.8 (2.1)
18	303.7	305.1	6.7	2.3 (2.3)
19	304.7	306.1	5.7	0.6 (1.9)
20	304.3	306.1	5.4	1.1 (2.0)
21	304.7	306.8	5.1	2.4 (2.1)
22	306.0	307.4	4.8	1.7 (1.6)
23	304.9	307.8	8.8	4.4 (4.7)

of 0.5 K, which implies an error of about 0.3 hPa in the computation of the pressure drop. Moreover, another possible source of error in our calculation is the fact that the circulation extends farther into the forest and the pasture than the two observation sites. Therefore, the observed pressure drop is smaller than the maximum pressure drop between the two regions. We plan to test this idea with data from a future field experiment.

Table 2 displays the observed values of the near-surface air temperature (averaged over 1 h) over the forest and the pasture, the thermodynamic efficiency, and the nonhydrostatic pressure drop between the forest and the pasture at 1400 LT for each day of the field experiment. The “observed” thermodynamic efficiency was derived from soundings over the pasture. The value of the nonhydrostatic pressure drop predicted by our theory is indicated between parentheses. The pressure drop is greatest when the boundary layer depth is near the maximum observed value and the air temperature difference between the pasture and forest sites is the largest, that is, on 23 August.

We now discuss the influence of the depth of the boundary layer on the thermodynamic efficiency of the mesoscale circulation. Figure 5 shows the potential temperature profile over the pasture (where the convective boundary layer is deeper) for 14 (dashed line) and 23 August (full line). 14 August is a day of shallow boundary layer. Accordingly, Fig. 4 shows that on this day the observed nonhydrostatic pressure drop between the forest and the pasture is only about 2 hPa. 23 August is the day of deepest boundary layer and on this day the nonhydrostatic pressure drop is the largest observed during RBLE 3. Moreover, the difference of the near-surface air temperature between the forest and the pasture is not large on 14 August ( $\Delta T_{na} \approx 3.1$  K) but near its maximum value on 23 August ( $\Delta T_{na} \approx 4.3$  K). This explains the large difference in the nonhydrostatic pressure drop observed on these two days.

In order to estimate the magnitude of the wind speed predicted by the heat engine theory independently of

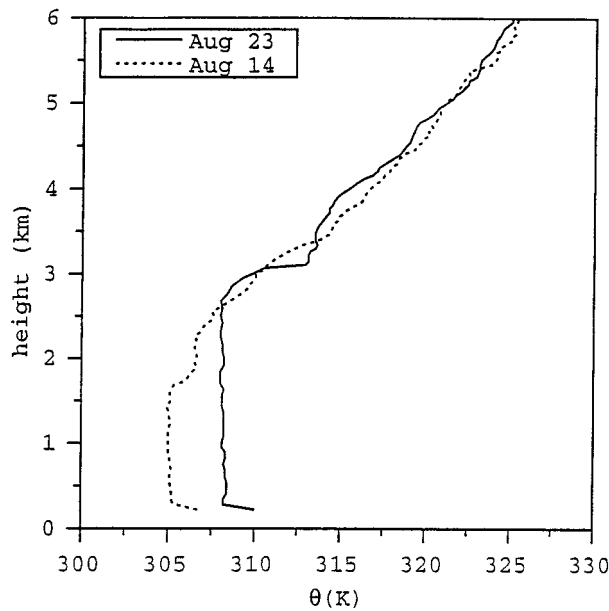


FIG. 5. Observed potential temperature profiles over the pasture at 1400 LT on 14 and 23 Aug.

the pressure perturbation, Eq. (18) is used to compute the intensity of the forest–pasture breeze. Taking typical values of  $\Delta T_{na} \approx 3$  K,  $\eta \approx 0.06$ , and  $\mu \approx 30$  (see Rennó et al. 1998), we get  $|\mathbf{v}| \approx 2.5$  m s<sup>-1</sup>. It follows from Fig. 3 that the observed wind perturbation is about 1.5 m s<sup>-1</sup>. Thus, the calculated perturbation wind speed is a bit higher than the observed value. Besides the fact that the perturbation wind speed is subject to a measurement error of about 1.0 m s<sup>-1</sup>, we argue that this difference might be due to the fact that the dimensionless coefficient of friction ( $\mu$ ) is underestimated. This in turn is due to the fact that the circulation path length ( $\sim 100$  km) is much larger than the depth of the convective layer (see Rennó et al. 1998).

Since the difference in elevation between the forest and the pasture sites is only 140 m ( $\Delta T_{ad} \approx 1.4$  K), the data from the RBLE 3 experiment might not be suitable to fully test the effects of terrain elevation on the nonhydrostatic pressure drop in sloping terrains. Thus, we use data of a field experiment on sea breezes in a sloping terrain to better test these effects. The field experiment occurred in February 1989 in the southeast region of Brazil (see Silva Dias and Machado 1997). We use data from two sites, one in São Paulo and another in Santos. While the Santos site is at 15-m altitude and is on the coast, the São Paulo site is at 802-m altitude and is located at about 60 km to the northwest of Santos. Silva Dias and Machado (1997) describe the topography of the region and the weather conditions during the experiment.

Table 3 shows the nonhydrostatic pressure drop between São Paulo and Santos observed at 1500 LT from 15 to 25 February 1989. We choose to present the values

TABLE 3. Observed values of the near-surface air temperature, the thermodynamic efficiency, and the nonhydrostatic pressure drop between Santos (site a) and São Paulo (site b) at 1500 LT. The data were collected between 15 (day 15) and 25 Feb (day 25) 1989. The “observed” thermodynamic efficiency was derived from the observed sounding over São Paulo. The value of the nonhydrostatic pressure drop predicted by our theory is indicated between parentheses. Note that  $T_a > T_b$ , except for day 15.

Day	$T_a$ (K)	$T_b$ (K)	$\eta$ (%)	$\Delta p$ (hPa)
15	297.7	298.6	2.3	1.8 (2.2)
16	304.5	301.0	4.6	1.4 (2.1)
17	303.7	301.2	3.6	1.4 (2.0)
18	301.2	297.5	2.3	1.3 (1.0)
19	301.7	299.0	2.6	2.6 (1.7)
20	302.5	301.0	3.9	1.7 (2.7)
21	305.9	301.8	3.3	0.2 (0.7)
22	304.8	301.0	2.3	-0.8 (1.0)
23	304.3	299.8	5.0	1.0 (1.6)
24	303.6	302.4	3.9	1.6 (2.8)
25	299.8	295.0	0.7	0.2 (0.2)

at 1500 LT because this is usually the time of peak intensity of the sea breeze circulation. The nonhydrostatic pressure drops predicted by our theory are also displayed in Table 3. Note that the predicted pressure drops are of the same order as the observed values. Moreover, the predicted pressure drops track well with the observed values in most days. However, the reader should be warned that other weather systems may affect the pressure drop between the two sites (see Silva Dias and Machado 1997). Nevertheless, an important insight emerges from the present theory; as illustrated in Table 3, it shows that a positive temperature gradient is *not* a necessary condition for sustaining a valley–mountain circulation. According to our theory, the necessary condition for a valley–mountain circulation to occur is that the potential temperature gradient between the valley and the mountain be positive (e.g., a nonadiabatic temperature gradient).

## 5. Conclusions

We have proposed a simple theory for the intensity of mesoscale convective circulations forced by surface heterogeneities in sloping terrains. The theory shows that the nonhydrostatic pressure drop between the two regions is a function of the depth of the convective boundary layer (through the thermodynamic efficiency), the nonadiabatic temperature, and humidity differences between the two regions.

Our theory sheds light on the basic thermodynamical mechanism by which topographical features enhance convective circulations. It follows from the second law of thermodynamics that the surface heat flux is proportional to the temperature difference between the ground and the near-surface air. A convecting air parcel absorbs heat from the surface while moving toward the updraft, that is, from point *a* to point *b*. Over flat terrain, an air-parcel temperature increases as it moves toward

the updraft. Thus, when the ground temperature is uniform (no horizontal gradients), the surface heat flux decreases as an air parcel moves toward the updraft. However, when the ground has horizontal temperature gradients, the surface heat flux decreases less rapidly when an air parcel moves toward warmer terrain. Our theory suggests that this is the reason why a heterogeneous surface has the potential for producing more intense convective circulations than do homogeneous surfaces.

Our theory also explains why elevated terrains force convective circulations (e.g., a valley–mountain circulation). When topographical features are present, an air parcel moving upslope cools down while expanding. Thus, when the temperature of the mountain slope decreases less rapidly with height than the dry adiabatic lapse rate, the air parcel will continue absorbing heat while moving upward along the slope. Indeed, it is well known that, even for the same solar heat flux, the radiative–convective equilibrium temperature of the atmosphere over elevated terrains is higher than that in the free atmosphere over lower regions (Barry 1992; Molnar and Emanuel 1999). That is, the temperature of a mountain slope decreases less rapidly with height than the dry adiabatic value. In fact, Molnar and Emanuel (1999) showed that the radiative–convective equilibrium temperature of elevated terrains decreases by only about  $2 \text{ K km}^{-1}$ , while the dry adiabatic lapse rate is approximately  $10 \text{ K km}^{-1}$ . The above reasoning shows that topographical features force strong convective systems because they lead to a large heat input to the convective heat engine. Moreover, it suggests that both the height of cumulus cloud bases and of the top of convective boundary layers are greater over mountains because of the anomalously high sensible heat flux into upslope moving convective updrafts. Therefore, topographical features enhance the strength of convective circulations by increasing both the heat input and the thermodynamic efficiency of the convective heat engine. Finally, another important insight that emerges from our theory is the fact that a positive temperature gradient is *not* a necessary condition for sustaining a valley–mountain circulation. According to our theory the necessary condition for a valley–mountain circulation to occur is that the potential temperature gradient between the valley and the mountain be positive (e.g., a nonadiabatic temperature gradient).

*Acknowledgments.* We would like to thank The University of Arizona's Department of Atmospheric Sciences, FAPESP, and NSF for partially supporting this study. In particular, the second author (NOR) would like to thank NSF for supporting this research under Grant

ATM-9612674. Moreover, the first author (EPS) would like to thank CAPES-BRASILIA and the Universidade Federal da Paraíba for supporting his visit to The University of Arizona. Finally, we would like to thank Ms. Margaret S. Rae for reading the manuscript and making many useful suggestions, and Brian Auvine for drafting the figures.

#### REFERENCES

- Atkinson, B. W., 1981: *Meso-Scale Atmospheric Circulations*. Academic Press, 495 pp.
- Avisar, R., and R. A. Pielke, 1989: A parameterization of heterogeneous land-surface for atmospheric numerical models and its impact on regional meteorology. *Mon. Wea. Rev.*, **117**, 2113–2136.
- Barry, R. G., 1992: *Mountain Meteorology*, 2d ed. Rutledge, 402 pp.
- Cutrin, E., D. W. Martin, and R. Rabin, 1995: Enhancement of cumulus clouds over deforested lands in Amazonia. *Bull. Amer. Meteor. Soc.*, **76**, 1801–1805.
- Dalu, G. A., and R. A. Pielke, 1989: An analytical study of the sea breeze. *J. Atmos. Sci.*, **46**, 1815–1825.
- Emanuel, K. A., 1986: An air-sea interaction theory for tropical cyclones. Part I: Steady-state maintenance. *J. Atmos. Sci.*, **43**, 585–604.
- , 1989: Polar lows as Arctic hurricanes. *Tellus*, **41A**, 1–17.
- Gash, J. H. C., C. A. Nobre, J. M. Roberts, and R. L. Victoria, 1996: An overview of ABRACOS. *Amazonian Deforestation and Climate*, J. H. C. Gash, Ed., Oxford University Press, 1–14.
- Golitsyn, G. S., 1979: Simple theoretical and experimental study of convection with some geophysical applications and analogies. *J. Fluid. Mech.*, **95**, 567–608.
- Haltiner, G. J., and F. L. Martin, 1957: *Dynamical and Physical Meteorology*. McGraw-Hill, 470 pp.
- Mahrer, Y., and R. A. Pielke, 1977: A numerical study of the airflow over irregular terrain. *Contrib. Atmos. Phys.*, **50**, 98–113.
- Molnar, P., and K. A. Emanuel, 1999: Temperature profiles in radiative-convective equilibrium above surfaces at different heights. *J. Geophys. Res.*, **104**(D20), 24 265–24 271.
- Pielke, R. A., 1974: A three-dimensional numerical model of sea breeze over south Florida. *Mon. Wea. Rev.*, **102**, 115–139.
- , 1984: *Mesoscale Meteorological Modeling*. Academic Press, 612 pp.
- Rabin, R. M., S. Stadler, P. J. Wetzel, and D. J. Stensrud, 1990: Observed effects of landscape variability on convective clouds. *Bull. Amer. Meteor. Soc.*, **71**, 272–280.
- Rennó, N. O., and A. P. Ingersoll, 1996: Natural convection as a heat engine: A theory for CAPE. *J. Atmos. Sci.*, **53**, 572–585.
- , M. L. Burkett, and M. P. Larkin, 1998: A simple thermodynamical theory for dust devils. *J. Atmos. Sci.*, **55**, 3244–3252.
- Rotunno, R., 1983: On the linear theory of the land sea breeze. *J. Atmos. Sci.*, **40**, 1999–2009.
- Silva Dias, M. A. F., and P. Regnier, 1996: Simulation of mesoscale circulations in a deforested area of Rondônia in the dry season. *Amazonian Deforestation and Climate*, J. H. C. Gash, Ed., Oxford University Press, 531–547.
- , and A. J. Machado, 1997: The role of local circulations in summertime convective development and nocturnal fog in São Paulo, Brazil. *Bound. Layer Meteor.*, **82**, 135–157.
- Staley, D. O., 1965: Radiative cooling in the vicinity of inversions and the tropopause. *Quart. J. Roy. Meteor. Soc.*, **91**, 282–301.